JOURNAL OF THE ROYAL SOCIETY Interface

The formation of a complex between calmodulin and neuronal nitric oxide synthase is determined by ESI-MS

Sally Shirran, Pierre Garnaud, Simon Daff, Derek McMillan and Perdita Barran

J. R. Soc. Interface 2005 **2**, 465-476
doi: 10.1098/rsif.2005.0055

JOURNAL OF THE ROYAL SOCIETY Interface

J. R. Soc. Interface (2005) **2**, 465–476
doi:10.1098/rsif.2005.0055
Published online 2 August 2005

The formation of a complex between calmodulin and neuronal nitric oxide synthase is determined by ESI-MS

Sally Shirran, Pierre Garnaud, Simon Daff, Derek McMillan and Perdita Barran†

School of Chemistry, University of Edinburgh, West Mains Road, Edinburgh EH9 3JJ, UK

Calmodulin (CaM) is an acidic ubiquitous calcium binding protein, involved in many intracellular processes, which often involve the formation of complexes with a variety of protein and peptide targets. One such system, activated by Ca^{2+} loaded CaM, is regulation of the nitric oxide synthase (NOS) enzymes, which in turn control the production of the signalling molecule and cytotoxin NO. A recent crystallographic study mapped the interaction of CaM with endothelial NOS (eNOS) using a 20 residue peptide comprising the binding site within eNOS. Here the interaction of CaM to the FMN domain of neuronal nitric oxide synthase (nNOS) has been investigated using electrospray ionization mass spectrometry (ESI-MS). The 46 kDa complex formed by CaM–nNOS has been retained in the gas-phase, and is shown to be exclusively selective for CaM.4Ca^{2+}. Further characterization of this important biological system has been afforded by examining a complex of CaM with a 22 residue synthetic peptide, which represents the linker region between the reductase and oxygenase domains of nNOS. This nNOS linker peptide, which is found to be random coil in aqueous solution by both circular dichroism and molecular modelling, also exhibits great discrimination for the form of CaM loaded with 4[Ca^{2+}]. The peptide binding loop is presumed to be configured to an α-helix on binding to CaM as was found for the related eNOS binding peptide. Our postulate is supported by gas-phase molecular dynamics calculations performed on the isolated nNOS peptide. Collision induced dissociation was employed to probe the strength of binding of the nNOS binding peptide to CaM.4Ca^{2+}. The methodology taken here is a new approach in understanding the CaM–nNOS binding site, which could be employed in future to inform the specificity of CaM binding to other NOS enzymes.

Keywords: ESI-MS; calmodulin; CaM–nNOS complex

1. INTRODUCTION

Electrospray ionization mass spectrometry (ESI-MS) has rapidly become an established and important technique with which to analyse non-covalent complexes in a solvent free environment. The 'softness' of desolvation and ionization allows complexes present in solution to resist the dissociation process and survive intact into the gas-phase. Several non-covalently bound systems have been studied by ESI-MS including DNA–protein (Xu *et al.* 1999), protein–metal (Taylor *et al.* 2001), protein–ligand (Bruce *et al.* 1998) and protein–protein (Robinson 2002). In addition the technique has been used to screen ligands from combinatorial libraries (Wigger *et al.* 2002) and for competitive binding of inhibitors (Smith & Whitesides 1995). Whether these gas-phase complexes relate to solution phase complexes and structures is still a matter of debate. Both results that correlate between gas-phase and solution phase (McLafferty *et al.* 1998) and results that contrast (Rogniaux *et al.* 1999) have been published. However it is generally agreed that ESI-MS is a powerful tool that can provide information on complexes which at the very least, compliments data achieved by other structural methods.

ESI-MS of biological samples typically employs solution conditions, comprising an organic solvent and low pH, to aid desolvation and protonation of the sample. However, these conditions can destroy the tertiary, and to some degree secondary structure of the protein and non-covalent complexes are unlikely to be preserved (Jarrold 2000). Furthermore, these conditions are far removed from most physiological environments, and therefore results cannot be readily correlated or compared to what may be happening *in vivo*. Therefore, to analyse non-covalent complexes, the sample is introduced from an aqueous solution, buffered to a relevant physiological pH.

†Author for correspondence (perdita.barran@ed.ac.uk).

Received 25 July 2004
Accepted 1 June 2005

ESI-MS has been used here to study the ubiquitous intercellular protein Calmodulin (CaM). CaM interacts with an impressive number of proteins, with a wide physiological diversity (Hoeflich & Ikura 2002), which have a broad biological role in the body. CaM binding proteins can be categorized into six groups (Chin & Mearns 2000).

(i) Proteins which bind irreversibly to CaM irrespective of Ca^{2+}. An example is phosphorylase kinase, an enzyme which requires denaturing conditions to dissociate CaM but is activated in the presence of Ca^{2+}.
(ii) Proteins which bind to apo CaM but dissociate reversibly in the presence of Ca^{2+}. Examples of this group are neuromodulin and neurogranin which might serve as intercellular reservoirs for CaM at resting concentrations of Ca^{2+}, but liberate Ca^{2+} activated CaM in response to elevated Ca^{2+}.
(iii) Proteins which form low affinity, inactive complexes with CaM at low concentrations of Ca^{2+}, when the Ca^{2+} sites of CaM are empty or partially occupied. At greater concentrations of Ca^{2+}, these proteins engage in high affinity complexes with and are activated by CaM. Calcineurin and smooth muscle light chain kinase belong to this group.
(iv) Proteins which bind to CaM in the presence of Ca^{2+}, which then inhibits their function. This group includes enzymes such as select members of the G protein receptor kinases and well as the inositol (1,4,5) trisphophate receptor type 1.
(v) Proteins that exhibit a more conventional behaviour and are activated by CaM–Ca^{2+}, such as CaM dependant protein kinases I, II and IV, it is thought that nNOS, examined here, belongs to this group.
(vi) Proteins in which CaM binding promotes their regulation, for instance multimeric CaM kinase II, both the substrate and the catalytic subunits require CaM binding to promote intermolecular autophosphorylation.

CaM contains four EF hands, and each of these helix loop helix regions binds a calcium ion (Chattopadhyaya *et al.* 1992; Kuboniwa *et al.* 1995). Upon binding calcium ions, CaM undergoes significant structural changes, which culminate, on the addition of four calcium ions in the exposure of a long, highly flexible helix between two globular domains, which in turn become more compact and conserved (Chattopadhyaya *et al.* 1992). As clear from the list above, it is in this metal bound conformation that CaM is most commonly found to interact with enzymes and proteins.

Previous work indicates that under certain ESI-MS conditions, CaM can also preferentially retain these four specific calcium ions (and hence conserve the calcium binding sites) in the gas-phase (Nemirovskiy *et al.* 1997). Biophysical studies have shown a number of additional divalent cation binding sites (Milos *et al.* 1989) and metals binding to these auxiliary sites have also been observable by mass spectrometry (Lafitte *et al.* 1995). Several ESI-MS studies have examined CaM in association with certain enzyme targets (Nemirovskiy *et al.* 1997; Moorthy *et al.* 2001; Nousiainen *et al.* 2003; Schulz *et al.* 2004), although for large systems, a short peptide which forms the *presumed* CaM binding site has been utilised (Lafitte *et al.* 1995) rather than the entire CaM–enzyme complex.

One of many enzymes which form an activated complex with CaM, is neuronal nitric oxide synthase (nNOS). nNOS, along with eNOS (endothelial) and iNOS (inducible), is involved in producing NO in a variety of cells during immune response, as well as promoting signalling cascades in the cardiovascular, nervous and immune systems (Daff 2001). nNOS consists of an N-terminal oxygenase domain and a C-terminal reductase domain and the two domains are linked by a peptide. It is to this peptide that CaM can bind reversibly when it becomes activated by calcium (Vorherr *et al.* 1993). CaM binding activates nNOS (and eNOS), providing them with a rapid response mechanism during their participation in signalling cascades. In contrast iNOS, which produces NO to then engage in protein and DNA destruction, is expressed with CaM bound and this has been shown to be largely independent of calcium concentration (Daff 2003).

Here ESI-MS is employed to study the interaction of calmodulin and calcium, and the subsequent binding of the FMN domain of nNOS. Specifically, we examine the interactions between CaM and the proposed CaM binding region of nNOS (Aoyagi *et al.* 2003). This approach has been taken before using urea gel electrophoresis and fluorescence spectroscopy (Vorherr *et al.* 1993) and for the CaM–eNOS system, with X-ray crystrallography (Aoyagi *et al.* 2003), but never by ESI-MS. The dissociation of the complex by collision induced dissociation (CID) of CaM and the nNOS peptide yields insights into the structure and modes of binding of this biologically important system. The methodology taken here could be applied to site directed mutants of the nNOS–CaM binding interface to further probe the specific interactions.

2. EXPERIMENTAL PROCEDURES

2.1. Protein and peptide synthesis

Bovine calmodulin was prepared from *Escherichia coli* cells expressing the protein as described previously (Craig *et al.* 2002) and stored as a freeze dried solid. Calmodulin was dissolved in ultrapure water at 20 mg ml^{-1}. Approximately 100 µl was dialysed prior to analysis against 4 l ammonium acetate (10 mM, pH 6.8) using Slide-a-Lyser dialysis cassettes from Pierce (Pierce Biotechnology, Rockford, IL). To chelate calcium from CaM, 0.4 M EGTA was added to the dialysed fractions in the presence of 10 mM ammonium acetate. The sample was then passed along a 10DG column (Biorad Laboratories), and protein containing fractions pooled and concentrated on a spin cartridge concentrator. All glassware and plasticware were acid

washed with 2 M HCl and rinsed with ultrapure water to prevent calcium contamination.

The nNOS FMN domain comprising residues 695–946 of rat nNOS with bound CaM (CaM–nNOS) was obtained as 50 µl of 20 mg ml^{-1} in tris buffer (Garnaud *et al.* 2004). The sample was diluted in half with ultrapure water, to 350 µM. Prior to analysis 100 µl was dialysed against 4 l ammonium acetate (10 mM, pH 7.5) again using Slide-a-Lyser dialysis cassettes from Pierce.

Fmoc-based solid-phase peptide synthesis of the proposed calmodulin binding region of nNOS, the linker peptide, Ac-KRRAIGFKKLAEAVKFSAKLM-NH_2 (Aoyagi *et al.* 2003) was conducted manually, on a 0.1 mmol scale, using Rink amide resin (200–400 mesh) and employing 0.5 mmol (5 equiv.) of each Fmoc amino acid per coupling reaction and HBTU/HOBt as coupling reagents. Resin and standard Fmoc protected amino acids were purchased from Novabiochem. The average coupling time was 6 h and the reaction progress was monitored using LC-MS and the Kaiser ninhydrin test. After synthesis the N-terminal amino acid was capped with acetic anhydride (1 mmol) in the presence of catalytic *N*,*N*-dimethylaminopyridine (0.01 mmol). The peptide was then cleaved from the solid-support by treatment with 95% TFA, 2.5% H_2O, 2.5% ethanedithiol for 3 h and purified by reversed-phase HPLC and lyophilized to afford the product as white 'fluffy' solid. LC-MS was performed using a Phenomenex Luna C18 LC-MS column (2.1×50 mm) and a gradient of 5–95% acetonitrile containing 0.1% TFA over 25 min (flow rate of 0.2 ml min^{-1}). Semi-preparative HPLC was performed using a Phenomenex LUNA C18 column and a gradient of 10–90% acetonitrile containing 0.1% TFA over 50 min (flow rate of 3.0 ml min^{-1}).

2.2. Mass spectrometry

Measurements were taken on a Micromass QToF instrument (Micromass UK Ltd, Manchester, UK) equipped with a Z-spray nanoflow source. Gold/palladium plated borosilicate glass nanoelectrospray needles (Proxeon Biosystems A/S, Odense, Denmark) were used to spray the sample into the mass spectrometer. Source conditions were kept constant for all measurements and consisted of; capillary (needle) voltage 800–1200 V, cone voltage 50 V, at 80 °C. Q-ToF instruments mass spectrometers incorporate both a quadrupole and an orthogonal time of flight detector. When measuring the full m/z range of the sample, the quad was used in the RF-only mode as a wide bandpass filter. Ions then pass through the hexapole collision cell, which is pressurized to 10 psi with argon gas and pass into the ToF, where they are detected on a multichannel plate set at 2.9 kV. For CID, the injection voltage into the collision cell was increased in 5 V increments.

Data were collected using MassLynx software version 3.2. A Savitzky–Golay smoothing algorithm was applied to raw data spectra at peak width at one-half height. Data was then deconvoluted to represent true mass using the transform package supplied by MassLynx version 3.1. The instrument was calibrated daily prior to experiments using horse heart myoglobin (Sigma Aldrich).

2.3. Circular dichroism

Circular dichroism (CD) experiments were carried out on a Jasco J-810 Circular Dichroism Spectrometer. Samples of the nNOS peptide were diluted to 100 µM in the required solvent and analysed in a 0.5 mm cell. Spectra were acquired from 190 to 300 nm, at a scan rate of 5 nm min^{-1}.

2.4. Molecular modelling using the AMBER force field (Case et al. 2005)

The nNOS linker peptide was built using X-Leap (Case *et al.* 2005) according to the sequence given above. All amino acids were held at their physiological ionization states, generating a peptide with net charge +6. A simulated annealing procedure was employed for an initial gas-phase energy minimization of the structures. High temperature dynamics was performed at 800 K, followed by dynamics at decreasing temperatures according to an exponential cooling curve. At 0 K the candidate structure is subjected to minimization using a steepest descent approach followed by a conjugate gradient algorithm. The minimized structure is then used as the seed for the next run of high temperature dynamics. Candidate structures of 300 were generated of the nNOS peptide. The lowest energy structure obtained was then subjected to another simulated annealing cycle with the use of an implicit solvent model (Tsui & Case 2000). Both the lowest energy conformations achieved were subjected to dymanics at 300 K for 1 ns. All calculations were performed on an SGI Origin 200 which forms part of the EPIC biocomputing facility.[1] The lowest energy structures from this run are those discussed within the text. These structures were viewed and analysed using visualizing molecular dynamics (Humphrey *et al.* 1996).

3. RESULTS AND DISCUSSION

3.1. Denaturing and buffered conditions with and without calcium addition

Calmodulin was initially analysed under 'standard' acidic electrospray mass spectrometry conditions, in a 1 : 1 methanol : water solution with 1% acetic acid. The predominantly bi-nodal mass spectrum of positive ions is shown in figure 1*a*, where ions are observed in the range $20<z<6$. This exhibits a clear distribution centred at $z=+15$, a second at $z=+9$ and a third series around $z=+11$ is also apparent. This multi-nodal distribution of charges suggests several different structures existing in equilibrium in the solution and illustrates how ESI-MS can be used to assess protein conformations as a function of solvent conditions, as shown by several researchers (Lafitte *et al.* 1995; Jarrold 2000; Dobo & Kaltashov 2001). The deconvoluted mass obtained over several charge states was

[1] www.epic.ed.ac.uk.

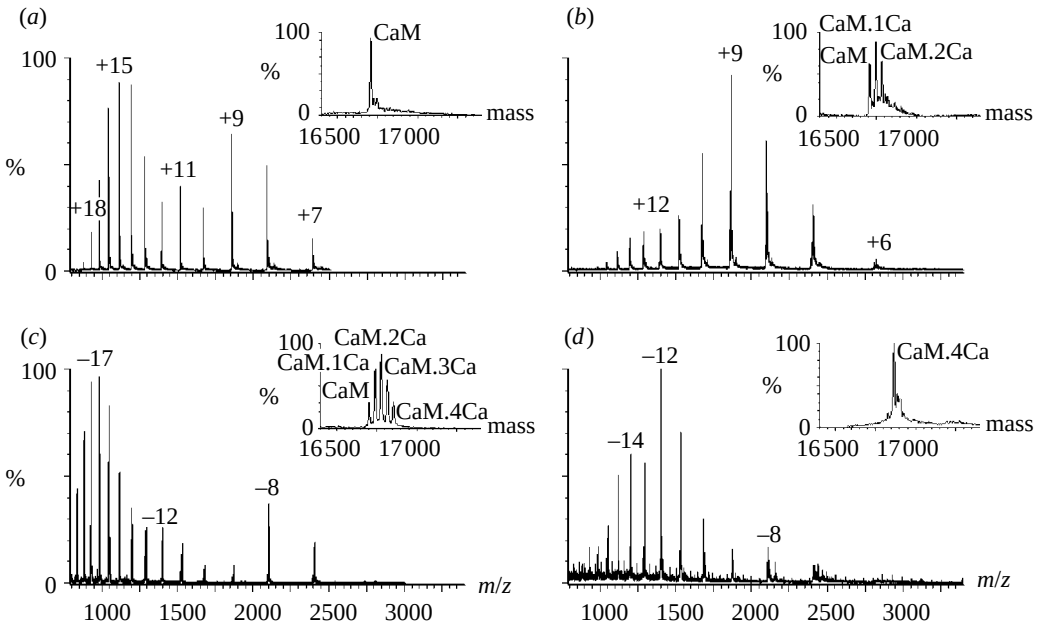

Figure 1. ESI-MS spectrum of 50 μM CaM in (*a*) 1 : 1 methanol : water and 1% formic acid, (*b*) ultrapure water, (*c*) 10 mM ammonium acetate (pH 6.8) and (*d*) 10 mM ammonium acetate pH 6.8 with addition of 100 μM calcium acetate. Insets show deconvoluted data obtained from each spectrum.

shown to be 16 706.6 Da, which is in excellent agreement with the theoretical average solution mass 16 706.45 Da.

The same sample was analysed in ammonium acetate (10 mM, pH 6.8) and water and the charge distributions acquired under these differing solvent conditions are shown in figure 1*b*,*c*, respectively. The predominantly single distribution, centred on $z=+9$ for the buffered solution, and at $z=+12$ in water, suggests that the number of conformations now present in solution has reduced compared to that obtained in acidic electrospray conditions (figure 1*a*). This is likely to be a narrow distribution around the folded native conformation, where less of the basic residues are available for protonation. Closer inspection of figure 1*b*,*c* shows more evidence for preservation of such a native structure. Deconvolution of all charges results in not only the mass of apo calmodulin at 16 706 Da, but four heavier species are apparent, at 16 744, 16 782, 16 820 and 16 858 Da (inset in figure 1*b*,*c*). These correspond to the addition of 1–4 calcium ions to the protein.

Ammonium acetate buffer was made with ultrapure water, but our calmodulin appears to have a limited *and* variable source of calcium ions, which despite careful acid washing of all glassware was difficult to eliminate totally. This inconsistency in background calcium levels is apparent by a comparison of the insets in figure 1*b*,*c* where the higher charge state series obtained when spraying from pure water actually yields an increased level of Ca^{2+} bound CaM, in contrast to the argument given above. This may also be due to buffer salts ligating at the Ca^{2+} binding sites up until desolvation is complete, thus preventing Ca^{2+} addition. The protein was subsequently analysed in 10 mM ammonium acetate with the addition of 100 μM calcium acetate, to provide a controlled level of calcium (figure 1*d*). Under these conditions the spectrum obtained has a similar charge distribution to figure 1*c*, tending towards lower charge states, again indicative of a more compact and folded structure (Jarrold 2000). Overall five species of calmodulin are found, corresponding to apo calmodulin and calmodulin with 1, 2, 3 or 4 calcium ions bound. No further additions of Ca^{2+} are seen suggesting the calcium addition is specific, for $n=4$ each EF hand being fully complexed with a bound calcium ion.

The work of several other researchers, including that reported in Lafitte *et al.* (1995), Nousiainen *et al.* (2003) also finds the stoichiometry of calcium binding to CaM in the gas-phase to be effectively similar to that existing in solution. However, there exists some controversy about the maximum number of calcium ions that may be bound to the protein, for example Lafitte *et al.* (1995) describe binding of up to 17 calcium ions, Gross and co-workers report up to 7 (Nemirovskiy *et al.* 1999), while Veenstra *et al.* (1997) observe a maximum of four. It is likely that this is due to the presence of varying concentration of free calcium in solution, and as stated on the website in footnote 1, the effect of source conditions on retention of auxiliary bound calcium ions.

To investigate this further, all calcium were chelated from the CaM sample using EGTA. Mass spectra were obtained with controlled and increasing amounts of calcium present. Figure 2 shows the number of calcium ions found bound to the calmodulin protein at a range of concentrations *up to and including* stoichiometric levels of CaM–Ca^{2+}. The CaM was present at 25 μM in all of these experiments; the points shown are taken from deconvolutions over the whole charge state envelope. As the concentration of calcium is increased the number of bound calcium ions also increases, until at a concentration ratio of 1 : 1 CaM–Ca^{2+}, CaM.4Ca^{2+} is the dominant species present. This is a somewhat surprising result, which suggests that a significant portion of the

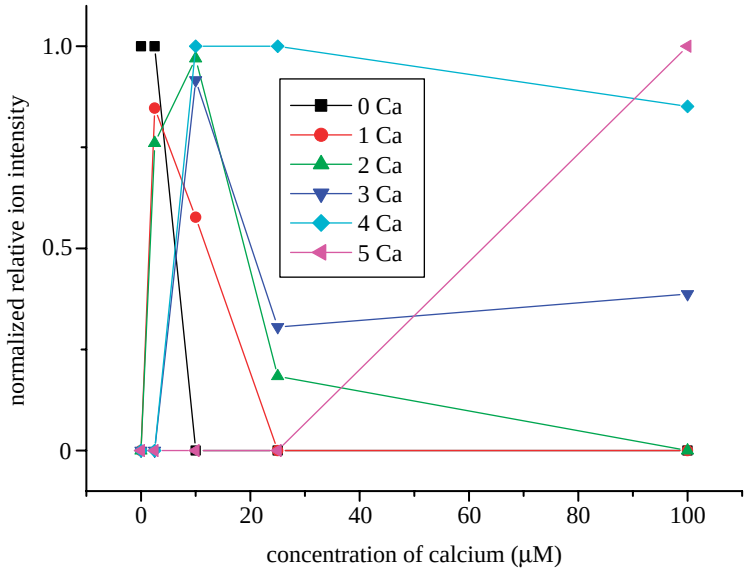

Figure 2. The population of CaM.nCa^{2+} species as a function of changing calcium ion concentration. Spectra were acquired in negative ionization mode, with the concentration of calmodulin maintained at 25 μM. The first spectrum were obtained post EGTA treatment of the protein, and then at the following μM concentrations of calcium acetate: 52; 5; 10; 25; 100. The points represent the intensity of the CaM.nCa^{2+} species, each normalized to the most intense peak in the spectrum.

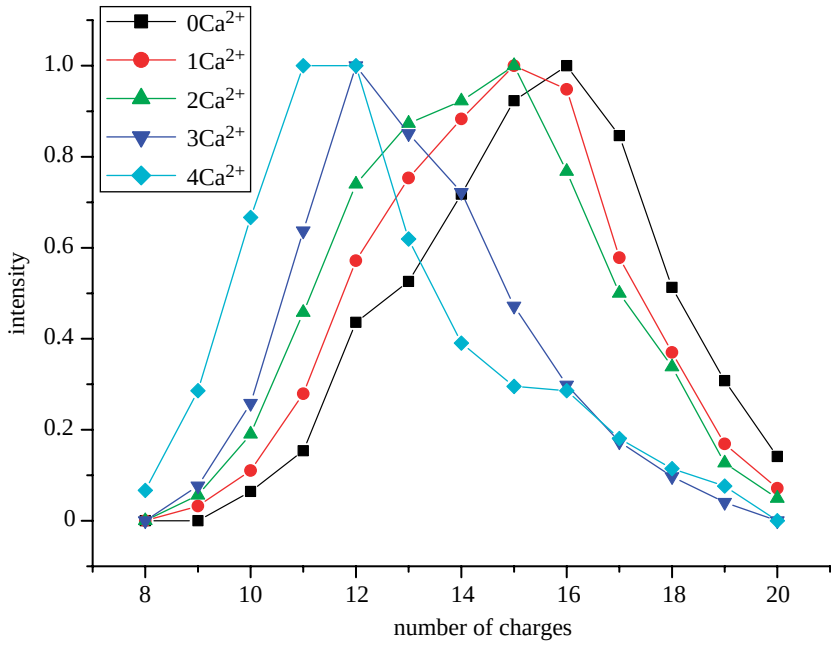

Figure 3. Charge states observed for each different species shown in figure 1*d*. The data has been normalized for each Ca containing species. At low charge states more Ca^{2+} is bound to CaM. Higher charge states are seen for CaM containing less Ca^{2+}.

protein present in solution is not being detected. One explanation for this is that we are presenting data here in negative ionization mode. We have avoided looking at the CaM.nCa^{2+} system in positive ionization mode, because in addition to CaM.nCa^{2+} species we also detect significant adduct sodium and potassium ions adducting to the calmodulin, presumably leached from the nanospray needles. This point has been made by Loo and co-workers (Hu *et al.* 1994), who also advocate examining CaM in negative ionization mode. Calmodulin is an acidic protein and over the pH range of 6–8 will be predominantly deprotonated. This is the state which then configures to calcium ions and/or to targets and so negative ionization conditions appear appropriate, although appears from the binding stoichiometry determined via ESI-MS as presented in figure 2, that this does not represent a full picture of the populations of CaM which must exist in solution.

Another explanation for this is that our protein concentration is not accurate; to measure it we have used an absorption co-efficient of CaM of 2900 M^{-1} cm^{-1} recorded at 276 nm, which we believe to be correct for human CaM which possess two tyrosine residues (Hans J. Vogel, Calgary University, private communication). Other values have been quoted the use of which, would alter the concentrations recorded here. From

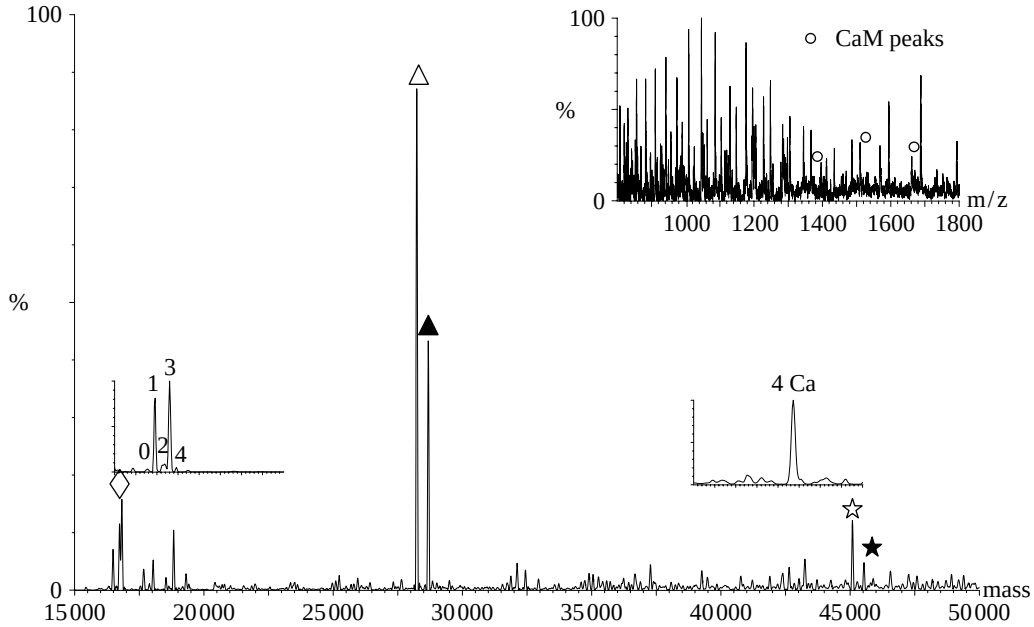

Figure 4. ESI-MS spectrum of 50 μM CaM and 50 μM of nNOS in 10 mM NH_4OAcM. In this spectrum, the open diamonds correspond to CaM with 0–4Ca^{2+}, the open triangles to the FMN domain of the nNOS complex, the black triangles to the FMN domain of the nNOS–FMN complex, the open stars to the FMN domain of the nNOS–CaM.4Ca^{2+} complex and the black stars to the FMN domain of the nNOS–FMN–CaM.4Ca^{2+} complex. In the inset which shows the undeconvoluted spectrum, the peaks corresponding to the calmodulin charged ion series are shown by open circles. Other peaks in this inset correspond to charged ion series from the protein nNOS, both with and without the FMN co-factor and also from the ensuing complex calmodulin. The high intensity low mass peaks are due to buffer ions and other sample impurities.

figure 2 it can be seen that the level of the CaM.4Ca^{2+} species falls at stoichiometric levels of calcium to CaM, and the CaM.5Ca^{2+} species starts to dominate. For this reason we record all of our CaM–complex spectra at a ratio of 1 : 2 CaM to Ca^{2+}.

The effect of calcium ions on the conformation(s) of calmodulin can also be seen in the ratio of calmodulin to calcium as a function of charge state. Figure 3 plots the different net charge states obtained for the different amounts of calcium incorporated into the protein at the ratio 1 : 2 CaM–Ca^{2+} which limits the uptake of calcium to 4 bound as discussed above. With no calcium ions the charge distribution is centred on −16, indicative of an open structure accessible to charging. However incorporating two calcium ions reduces this to −15, indicating the conservation into the gas-phase of a tighter structure than the apo form. This phenomenon continues up to 4 calcium ions where the distribution centres on $z=-11$, which coupled with the fact that the maximum number of specific calcium are bound suggests a much tighter structure. Narrowing charge states distributions of as a function of Ca^{2+} addition is also indicative of a more compact and less dynamic structure for the fully calcium loaded form. Such observations are in line with that reported by others investigating CaM using ESI-MS (Lafitte *et al.* 1995; Veenstra *et al.* 1997; Nemirovskiy *et al.* 1999; Nousiainen *et al.* 2001).

The effect of Ca^{2+} binding at each of the 4 sites in CaM has been investigated by several researchers (Cox *et al.* 1988). It is evident that there are two pairs of sites, which demonstrate 'paired co-operativity'. Those in the C-terminal domain have an affinity for calcium which is 10–15 times higher than that in the N-terminal domain, although absolute and even relative calcium affinities will vary according to the ionic strength of the liquid. The charge states series obtained for apo 1 and 2 calcium ions centres at $z=-15$ while those for 3 and 4 calcium ions at $z=-11$ to −12. It is tempting to speculate that this is symptomatic of calcium binding (or being retained) in the EF hands in the C-terminal domains in the higher charge states, and again this illustrates the structural information which can be gathered from analysis of ESI-MS data.

3.2. Complex with nNOS

Once configured with calcium, CaM is able to bind specifically to target proteins. Figure 4 shows the deconvoluted spectrum data of calmodulin with the nNOS protein, and the complex formed between them when sprayed at a ratio of 1 : 1. Raw data are shown in the inset in this figure. Calmodulin is here present in apo, and nCa^{2+} forms where $n=1$, 2, 3 and 4 and nNOS is observed at masses of 28 228 Da and with its bound cofactor (FMN) at 28 682 Da. All five species of CaM are available, however not all 5 species form complexes with nNOS, and only a single peak is seen at 45 090 Da. This corresponds to the mass of the complex with CaM.4Ca^{2+}. A peak is also seen for nNOS complexed to CaM.4Ca^{2+} with its bound cofactor (FMN) where the ratio's are the same as that obtained for the nNOS protein alone—the co-factor having no significant effect on the relative binding affinity. It is conceivable that the cofactor is lost from nNOS during the electrospray process, or that nNOS is present in solution with and without FMN, but nevertheless it does not appear critical to gas-phase complex stability.

That the protein binds exclusively to the $4Ca^{2+}$ form of calmodulin, suggests highly specific binding exists between CaM.$4Ca^{2+}$ and nNOS which has here been successfully retained in the gas-phase. The abundances of the isolated CaM isoforms are altered with respect to those shown in figure 1*d* (see lower right-hand side inset in figure 4). Remarkably there is very little free CaM.$4Ca^{2+}$, apparently it has been scavenged by the nNOS peptide, and correspondingly the abundance of CaM.$2Ca^{2+}$ is also low, due to the cooperativity of binding two calcium ions leading to fully calciated CaM.$4Ca^{2+}$. To our best knowledge this is the first CaM–enzyme complex that has been observed intact by ESI-MS.

3.3. Complex with nNOS peptide

The study of the complex was simplified by analysing only the CaM binding region of nNOS peptide. This allows for a more detailed analysis of the binding affinity in the gas-phase on our instrument. Figure 5 shows the raw data spectrum of 50 μM Calmodulin with 50 μM of nNOS peptide in 100 μM $Ca(OAc)_2$ and 1 mM NH_4OAc. Alongside the main series assigned to calmodulin, a second series, corresponding to the CaM–nNOS complex can clearly be seen.[2] As the concentration of the nNOS peptide is varied substoichiometrically, the amount of complex observed also decreases, at a ratio of 1 : 2 CaM–nNOS no increase in the intensity of complex peaks is apparent, suggesting a specific binding. This second series only corresponds to peptide addition to the CaM.$4Ca^{2+}$ form of the protein, as is apparent in the deconvoluted spectrum (inset in figure 5). Although all 5 species of calmodulin are present, a complex forms only with CaM.$4Ca^{2+}$. Furthermore, in the absence of calcium no complex was seen. The observed charge state distributions of the complex are different from that of the free CaM, as shown in figure 5, where the complex is observed in positive ionization mode, the peptide is only observed bound to CaM in charge states $z=7$–10, whereas CaM is seen in a range of charge states from $z=7$–18. In negative ionization mode (not shown) the complex is observable over the range $z=6$–10, which as may be seen from figure 3 is significantly narrower than for uncomplexed CaM.$4Ca^{2+}$.

These results may be contrasted with those obtained by Gross *et al.* who examined the CaM–melittin complex using ESI-MS (Nemirovskiy *et al.* 1997). For low Ca^{2+} concentration they obtained melittin binding to CaM.$2Ca^{2+}$, which was never here observed for the CaM–nNOS system either with the protein or the linker peptide. However with higher Ca^{2+} concentrations, they show a distinct preference for CaM.$4Ca^{2+}$. This suggests that melittin to CaM binding is less specific that that found here for the nNOS linker peptide, although their experimental source conditions are somewhat different. This is also confirmed by the narrower charge state distribution that we observe here for the CaM–nNOS peptide complex than that reported by Gross *et al.* for CaM–melittin. A recent study by Schulz *et al.* (2004) has also examined the CaM–melittin complex with mass spectrometry, but the resolution of the MALDI-ToF instrument they employed is not sufficient to elucidate stoichiometry of Ca^{2+} binding. Their cross-linking studies provide evidence for two modes of peptide binding to CaM, described as one parallel and one antiparallel. These findings are interesting and the experimental methodology novel, their analysis relies on comparisons to NMR structure data for (Ikura *et al.* 1992), and the MS studies *per se* do not discern the number of calcium ions present within the complex.

Structures have been obtained for calmodulin complexed with a peptide which constitutes the CaM binding site in the enzyme myosin light chain kinase (MLCK). Both the smooth muscle (Meador *et al.* 1992; crystal) and the skeletal muscle variants (Ikura *et al.* 1992; NMR) have been reported and these studies present the complex only in the presence of four calcium ions. Derrick and co-workers have examined this system via ESI FT–ICR-MS (Hill *et al.* 2000; Nousiainen *et al.* 2001, 2003) and were able to form a complex between apo calmodulin and the MLCK peptide. They suggest that the CaM–MLCK complex forms first and that calcium ions bind subsequently, perhaps cooperatively, Derrick's findings differ somewhat from the detailed biophysical work of Bayley *et al.* (1996) who have found the complex CaM.$2Ca^{2+}$, wherein the C-terminal EF hands have first been occupied is a necessary intermediate state prior to binding the target MLCK. Persechini *et al.* (1994), taking a similar approach to Bayley, investigate the binding of CaM domains to MLCK and nNOS. They find that the activity of MLCK enzymes is retained at 80% by binding C-terminal domains at the sites normally occupied by the C and N terminus, whereas nNOS activity under similar conditions is only 50% of normal levels. This signifies the relative importance of both CaM domains being available and in their calcium loaded form for stable nNOS complex formation.

Our findings illustrates the power of gas-phase techniques in interrogating the dynamics of complex formation, but also underlies the specificity of the CaM–nNOS complex, which was only observable in the presence of calcium and only formed a complex with CaM.$4Ca^{2+}$, both in its 'abbreviated' form as the linker peptide and with a substantial portion of the nNOS enzyme.

3.4. Collision induced dissociation of CaM–nNOS: positive ionization

Using the quadrupole as a mass selective analyser, single charge states of the complex were isolated for CID using argon in the collision cell; fragments were measured using the ToF analyser. The most dominant complex peaks here present at $z=+7$ and $+8$ were selected.

Figure 5*a*,*b* show isolation of these charge states and their dissociation arising as the collision voltage is increased. Voltages of 45 V were required to produce a

[2]Since all observed CaM complex ions are found with 4 calcium ions, we will simplify *complex*–CaM.$4Ca^{2+}$ to CaM–complex.

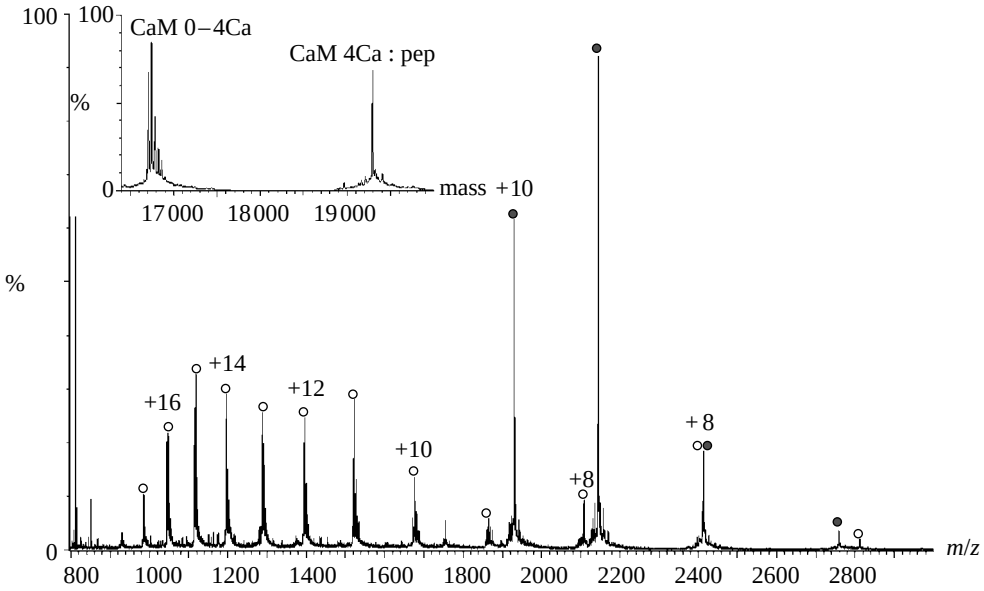

Figure 5. Nano-ES spectrum of the complex formed between CaM and the nNOS linker peptide. Charged ion series can be seen for free CaM (small open circles) as well as for the complex (filled circles). Inset shows the deconvoluted masses found, corresponding to five separate CaM species ($CaM.0Ca^{2+}$ through to $CaM.4Ca^{2+}$).

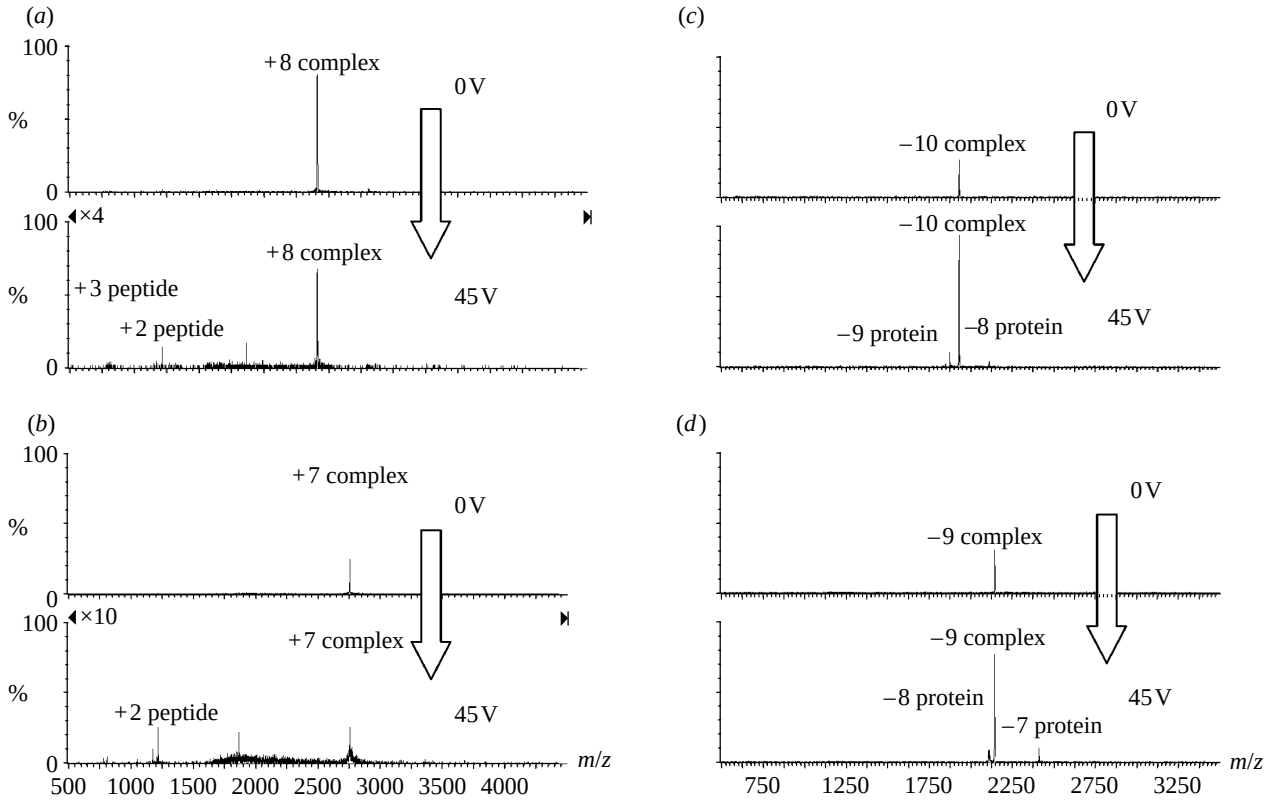

Figure 6. (*a*,*b*) Molecular models of the nNOS linker peptide obtained during molecular dynamics simulations at 300 K. (*a*) is a gas-phase structure and (*b*) arises from use of the Born Solvent model. (*c*) Crystal structure of the eNOS peptide as it is configured when complexed to CaM. Peptide backbones are represented by a ribbon, which is coloured according to the conformation presented: white, random coil; blue, turn; purple, α-helix. The residues which correspond to the principle recognition sites in CaM (according to the 1–5–8–14 motif) are shown as liquorice structures and labelled accordingly with their atoms represented in the standard colours.

significant amount of cleavage of nNOS peptide from the complex, higher injection energy than this resulted in complete loss of transmission of the complex or its dissociated constituents. Figure 5*a* shows the +8 charge state of CaM–nNOS losing the +3 charge state nNOS peptide and (for higher injection energies) the +2 charge state nNOS peptide. Similarly the +7 charge state dissociates with loss of +2 charge state nNOS peptide. In both cases this suggests that the +5 charge state of the protein is retained. However, this is

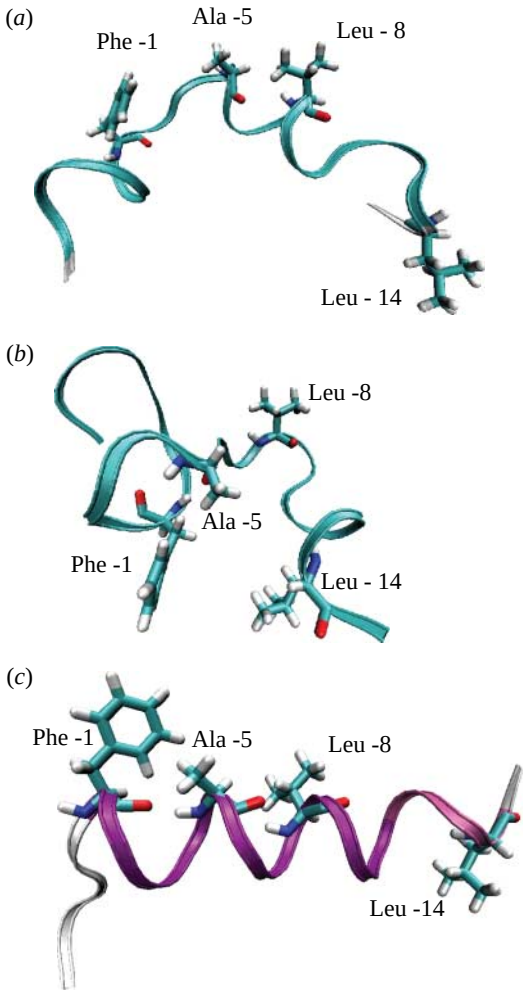

Figure 7. Products of dissociation of the isolated charge states ions of the CaM–nNOS peptide complex. In each figure the top spectrum shows the isolation of the respective charge state and the bottom figure the related dissociation products at 45 collision volts with 10 psi argon in the collision cell. (*a*) +8 charge state, (*b*) +7 charge state, (*c*) top: −10 charge state and (*d*) −9 charge state.

not seen in either dissociation spectra, which may be due to the fact that +5 calmodulin (3374.2 m/z) would appear in a region of the analyser where peak intensity is always poor. The +6 charge state would be expected to be observable as a dissociation partner (see figure 1*c*,*d*) to the +2 nNOS peptide from the +8 parent, this is also not observed. However, this is a process that occurs only at high injection energies and it is probable that charge stripping occurs to the +8 complex reducing it to the +7 complex which will then dissociate to +5 protein and +2 peptide (as shown in figure 5*b*). This is supported by the small peak to the right of the +8 complex peak in the top spectrum of figure 5*a* which is attributed to +7 CaM–nNOS, since it is present as a charge stripped product even at 0 V injection energy this provides a plausible route for the lack of +6 CaM as a product ion.

Analogous experiments have been performed by Derrick and co-workers on the CaM–MLCK complex (Hill *et al.* 2000; Nousiainen *et al.* 2001, 2003). These studies, which employ FT-ICR MS, show in source dissociation of the complex ions with +8 and +7 charge states into +2 peptide and +6 and +7 protein, and at higher energies into +3 peptide and +5 protein. An explanation of these results is also that the +5 protein appears as a dissociation product from the +7 complex ion as we observe for the CaM–nNOS system. The conclusion from the CID results of Nousiainen *et al.* (2003) is that the complex interaction is mediated by at least one salt bridge; the resolution available to these workers allows the proton transfer process to be unambiguously assigned.

3.5. Collision induced dissociation of CaM–nNOS: negative ionization

The experiment described above was also performed on deprotonated species and similarly the most intense peaks (here −10 and −9) were selected for isolation. The fact that the protein in each case is also carrying +8 charges from the four Ca^{2+} ions suggests that the complex ions observed with $z=-9$ and −10, the complex possesses −17 and −18 deprotonated acidic residues, some of which may be present at the binding site. Figure 5*c*,*d* shows the isolation of −10 and −9 charges states, respectively, and the dissociation products observed as the collision voltage is increased. Compared to the positive ionization CID the complexes here appear much more stable and less resistant to dissociation, even at high injection energies which suggests a different structural form to the complex ion formed from positive ESI compared with negative ESI. The dissociation of the −10 complex shows −9 and −8 protein, implying a corresponding peptide product with $z=-1$ or −2. The same occurs with dissociation of the −9 complex which dissociates to −8 and −7 protein, again suggesting loss of the peptide with a −1 and −2 charge. In both cases the protein retains all of its bound calcium ions, which is consistent with the findings of Derrick and co-workers (Nousiainen *et al.* 2003) for low energy in source dissociation of the CaM–MLCK complex, although at higher collision energies they do observe breakup of the CaM.4Ca^{2+} complex.

No signals are seen corresponding to negatively charged nNOS peptide product ions. The peptide is very basic with only one acidic side chain, and it is difficult to observe as a deprotonated ion. The effective decrease in the charge state of the complex to form CaM products must be due to proton transfer from the nNOS peptide product, potentially forming a neutralized carboxylic group on CaM. For nNOS peptide this leaves an unobservable neutral species implying that binding at the CaM–nNOS interface is via at least one salt bridge interaction in the gas-phase. This observation has been made by Getzoff and co-workers (Aoyagi *et al.* 2003) for the eNOS linker peptide, where strong interactions are present between the basic residues at the N terminus and several glutamic acid residues in CaM. In addition they describe a hydrophobic pocket created around methionine residues in CaM which is configured by specific residues in the (NOS) linker peptide binding loop. To examine the likely configuration of the nNOS peptide we have employed molecular mechanics based calculations.

3.6. nNOS peptide conformation via molecular modelling and circular dichroism

The low energy structures of nNOS peptide obtained using the Amber force field are shown in figure 6*a* (gas-phase) and figure 6*b* (born solvent). These are both representative snapshots taken from 1 ns dynamics runs. nNOS peptide is signified by the peptide backbone, with residues 7, 10, 12, 18 (Phe, Ala, Val, Leu) which are those thought to be primarily involved in the interaction with CaM (Aoyagi *et al.* 2003) depicted by liquorice representations. The gas-phase low energy structures were all elongated with separated N and C termini, while the Born solvent model structures tended to more compact globular conformations. As shown in figure 6*a*, gas-phase structures exhibited some helicity, presenting the first three residues proposed (according to the generalized calcium dependent 1–5–8–14 motif; Rhoads & Friedberg 1997) to interact with the central linker α-helix of CaM along one face and the fourth residue on the opposite side. This binding motif is analogous to that found with MLCK (Ikura *et al.* 1992; Nousiainen *et al.* 2001) and is identifiable by (ideally) 12 amino acid residues flanked by two bulky hydrophobic residues. The nNOS peptide examined here also exhibits this classic motif, where the first hydrophobic residue is phenalyamine (1) and the last leucine (14). The additional hydrophobic amino acids found at positions five and eight further stabilize binding to CaM. If these are presented in a plane within the peptide/protein target they will form favourable hydrophobic interactions with CaM.

Figure 6*c* shows the eNOS peptide from the crystal structure of the CaM–eNOS complex as solved by Getzoff and co-workers (Aoyagi *et al.* 2003), again the residues mapped to interact with CaM are illustrated by liquorice representations. While our gas-phase molecular model of nNOS peptide does not overlay to the eNOS, it is apparent that the peptide in the FMN CaM binding domain that we synthesized, has the propensity to form a helix, which in turn offers the correct proposed residues for the hydrophobic interactions with CaM. We believe that more rigorous conformational searching, (which is beyond the computational resources presently available to us) could generate a more configured helical peptide. An alternative route would be to employ homology modelling with the eNOS peptide as configured to CaM as a starting structure. It is clear that the solvent model did not generate a helical structure, and so it appears that CaM configures a random coil nNOS peptide on binding. The gas-phase conditions which generated the nNOS structure in figure 6*a* are probably more similar to the lower dielectric medium it will experience when complexed to CaM, if the binding is comparable to that for CaM–eNOS where the protein 'wraps' around the peptide.

In order to further check the helical nature of nNOS peptide we employed CD. The peptide was analysed in 10 mM ammonium acetate to provide similar conditions as used for mass spectrometry experiments. Under these conditions nNOS peptide adopted a coil formation (see electronic supplementary material). However, when bound to calmodulin, as stated above, it is presumed that the peptide will not be solvated by water and would essentially be in a hydrophobic environment with a significantly lower dielectric constant. To mimic this, the linker peptide was analysed in methanol where it did indeed form a helical structure (data not shown). The caveat to this finding is that many peptides of this length will form random coil structures in solution and could then form helical structures in less aqueous media, or in the gas-phase. Formation of this secondary structure by the nNOS peptide compliments the findings of Getzoff and co-workers (Aoyagi *et al.* 2003) for the eNOS linker peptide which is shown to be helical in complex formation with CaM (figure 6*c*). These physical investigations imply that this region of the FMN domain of nNOS contains a peptide loop with a helical propensity. We believe, while unstable in solution, this helix is stabilized on complex formation with CaM4.-Ca^{2+} as shown from our mass spectrometry studies.

4. CONCLUSIONS

This work has shown that more information can be taken from mass spectrometry than simply molecular mass. The degree of charging seen on the protein and its complexes has provided insights into the structure which correlate well with information from other analytical techniques. Our use of CID and complementary techniques have further interrogated this system allowing us to outline a number of important observations about the CaM–nNOS complex, as follows.

(i) Solution conditions alter the range of conformations available to the protein; analysis of the charge state distributions indicates that mass spectrometry can be employed to examine co-operative binding of metal ions at different sites within the protein.
(ii) The specificity of the technique has been highlighted by the targeted binding of nNOS peptide to CaM.4Ca^{2+}.
(iii) We have confirmed the proposed CaM binding site in nNOS peptide as residues Lys730–Met750 via the specific binding of the synthesized nNOS peptide to CaM.4Ca^{2+}.
(iv) CID yields charged products of both the protein and peptide which indicate that gas-phase binding is partly mediated via electrostatic salt bridge interactions, although we expect hydrophobic interactions to be dominant.
(v) This peptide is found to be helical in hydrophobic conditions such as those presented on CaM binding. Molecular modelling of the peptide in the gas-phase produces a helix which corresponds to that found in the crystal structure of eNOS–CaM.

If the CaM recognition and binding by nNOS is similar to that postulated by Getzoff for eNOS, then the residues responsible for interaction will align along one side of the linker peptide. Our model of the nNOS peptide certainly displays this. Additionally our experimental work demonstrates that this peptide exhibits

exclusive selectivity for the fully calcium loaded form of CaM which is the configured conformation required to accept the binding domain presented by nNOS. It appears likely that nNOS exhibits the classic 1–5–8–14 Ca^{2+} dependent binding motif (Rhoads & Friedberg 1997) where here 1 corresponds to residue 7 (Phe) in the nNOS peptide. Our observation (figure 6*a*) that the fourth residue in this motif does not lie along the same plane as the first three is also consistent with the findings of Getzoff *et al.* who state that this last key hydrophobic residue lies outside of the interior created by holo-CaM as it complexes.

We present evidence from CID that electrostatic salt bridge interactions are present at the binding site and are subsequently ruptured as the complex breaks up. This is proved by the charge reduction that occurs when the CaM product is detected as a negative ion (figure 7) which must correspond to proton transfer from nNOS peptide to the protein. Gas-phase complex binding will favour electrostatic above hydrophobic interactions (Robinson *et al.* 1996), although the hydrophobic crevice formed by the rearrangement of the helices of CaM on binding to the nNOS target (Aoyagi *et al.* 2003; Schulz *et al.* 2004) and the 1–5–8–14 motif presented by nNOS mean that hydrophobic interactions must play a dominant role in peptide binding. Since it is apparent that the N-terminal section of the nNOS peptide interacts with glutamic acid groups in the protein (Aoyagi *et al.* 2003), we conclude that proton transfer is likely to occur here, especially since this is likely to be not too deeply embedded in the protein. It is possible that the interactions involved in the complex obtained under positive ionization conditions are somewhat different, there may be less deprotonated glutamic acid residues available for the electrostatic interactions, and hence charge is retained on basic residues on the peptide during dissociation. Future work could investigate this by mutating out selective residues on the nNOS peptide or by taking the approach of Gachhui *et al.* (1997) and Kondo *et al.* (1999), who employ mutated calmodulin chimeras to determine the effect of altering the complex interface on NOS activity. Our findings differ from those of Derrick and co-workers for the peptide complex formed between CaM and the target site in MLCK which also follows the 1–5–8–14 paradigm (Hill *et al.* 2000; Nousiainen *et al.* 2003), and also from those of Gross *et al.* with melittin (Nemirovskiy *et al.* 1997). Both of these systems have been shown by mass spectrometry to form complexes which are not dependent on four calcium ions sequestering to CaM, whereas in our hands the nNOS system is only observable bound to the $4Ca^{2+}$ loaded form of calmodulin.

The work presented here shows for the first time an isolated gas-phase complex between the FMN domain of nNOS and calmodulin. We have used a variety of techniques to probe the structure and strength of binding of this biologically active system, and we believe that studies of this nature will have increased importance since they utilise relatively low amounts of protein and have the potential to interrogate binding interactions in microscopic detail.

We thank Dr Lyndsey Sawyer and Lynsey Mack for useful discussion on circular dichroism and the use of the spectrometer. The EPIC Biocomputing facility is acknowledged for the use of their facilities. We thank The School of Chemistry, The University of Edinburgh for the award of a studentship to S.S. and the use of the QTOF mass spectrometer. The EPSRC are gratefully acknowledged for the award of an advanced research fellowship to P.B. and financial support of these studies.

REFERENCES

Aoyagi, M., Arvai, A. S., Tainer, J. A. & Getzoff, E. D. 2003 Structural basis for endothelial nitric oxide synthase binding to calmodulin. *EMBO J.* **22**, 766–775.

Bayley, P. M., Findlay, W. A. & Martin, S. R. 1996 Target recognition by calmodulin: dissecting the kinetics and affinity of interaction using short peptide sequences. *Protein Sci.* **5**, 1215–1228.

Bruce, J. E., Smith, V. F., Liu, C., Randall, L. L. & Smith, R. D. 1998 The observation of caperone-ligand noncovalent complexes with ESIMS. *Protein Sci.* **7**, 1180–1185.

Case, D. A. *et al.* 2005 Amber 7 http://amber.scripps.edu/.

Chattopadhyaya, R., Meador, W., Means, A. & Quiocho, F. 1992 Calmodulin structure refined at 1.7 angstrom resolution. *J. Mol. Biol.* **228**, 1177–1192.

Chin, D. & Mearns, A. R. 2000 Calmodulin: a prototypical calcium sensor. *Trends Cell Biol.* **10**, 322.

Cox, J. A., Comte, M., Mamar-Bachi, A., Milos, M. & Schaer, J. J. 1988 Cation binding to calmodulin and relation to function. In *Calcium and calcium binding proteins: molecular and functional aspects* (ed. C. Gerday, L. Bolis & R. Gilles), pp. 145–147. New York: Springer.

Craig, D. H., Chapman, S. K. & Daff, S. 2002 Calmodulin activates electron transfer through neuronal NO synthase reductase domain by releasing an NADPH-dependent conformational lock. *J. Biol. Chem.* **277**, 33 987–33 994.

Daff, S. 2001 Control of electron transfer in neuronal NO synthase. *Biochem. Soc. Trans.* **29**, 147–152.

Daff, S. 2003 Calmodulin-dependent regulation of mammalian nitric oxide synthase. *Biochem. Soc. Trans.* **31**, 502–505.

Dobo, A. & Kaltashov, I. A. 2001 Detection of multiple protein conformational ensembles in solution via deconvolution of charge-state distributions in ESI MS. *Anal. Chem.* **73**, 4763–4773.

Gachhui, R., Abu-Soud, H. M., Ghosha, D. K., Presta, A., Blazing, M. A., Mayer, B., George, S. E. & Stuehr, D. J. 1997 Neuronal nitric-oxide synthase interaction with calmodulin troponin C chimeras. *J. Biol. Chem.* **10**, 5451–5454.

Garnaud, P. E., Koetsier, M., Ost, T. W. & Daff, S. 2004 Redox properties of the isolated FMN- and FAD-binding domains of neuronal NO synthase. *Biochemistry* **43**, 11 035–11 044.

Hill, T. J., Lafitte, D., Wallace, J. I., Cooper, H. J., Tsvetkov, P. O. & Derrick, P. J. 2000 Calmodulin–peptide interactions: apocalmodulin binding to the myosin light chain kinase target-site. *Biochemistry* **39**, 7284–7290.

Hoeflich, K. P. & Ikura, M. 2002 Calmodulin in action: diversity in target recognition and activation mechanisms. *Cell* **108**, 739.

Hu, P., Ye, Q.-Z. & Loo, J. A. 1994 Calcium stoichiometry determination for calcium binding proteins by electrospray ionization mass spectrometry. *Anal. Chem.* **66**, 4190–4194.

Humphrey, W., Dalke, A. & Schulten, K. 1996 VMD: visual molecular dynamics. *J. Mol. Graph.* **14**, 33–38.

Ikura, M., Clore, G. M., Gronenborn, A. M., Zhu, G., Klee, C. B. & Bax, A. 1992 Solution structure of a calmodulin-target peptide complex by multidimensional NMR. *Science* **256**, 632–638.

Jarrold, M. F. 2000 Peptides and Proteins in the vapour phase. *Annu. Rev. Phys. Chem.* **51**, 179–207.

Kondo, R., Tikunova, S. B., Je Cho, M. & Johnson, J. D. 1999 A point mutation in plant calmodulin is responsible for its inhibition of nitric-oxide synthase. *J. Biol. Chem.* **51**, 36 213–36 218.

Kuboniwa, H., Tjandra, N., Grzesiek, S., Ren, H., Klee, C. B. & Bax, A. 1995 Solution structure of calcium-free calmodulin. *Nat. Struct. Biol.* **2**, 768–776.

Lafitte, D., Capony, J. P., Grassy, G., Haiech, J. & Calas, B. 1995 Analysis of the ion binding sites of calmodulin by ESI-MS. *Biochemistry* **34**, 13 825–13 832.

McLafferty, F. W., Guan, Z., Haupts, U., Wood, T. D. & Kelleher, N. L. 1998 Gaseous conformational structures of cytochrome c. *J. Am. Chem. Soc.* **120**, 4732–4740.

Meador, W. E., Means, A. R. & Quiocho, F. A. 1992 Target enzyme recognition by calmodulin: 2.4 A structure of a calmodulin–peptide complex. *Science* **257**, 1251–1255.

Milos, M., Comte, M., Schaer, J. J. & Cox, J. A. 1989 Evidence for 4 capital and 6 auxiliary cation binding sites on calmodulin: divalent cations interactions monitored by direct binding and microcalorimetry. *J. Inorg. Biochem.* **36**, 11–25.

Moorthy, A. K., Singh, S. K., Gopal, B., Surolia, A. & Murthy, M. R. N. 2001 Variability of calcium binding to EF-hand motifs probed by ESI-MS. *J. Am. Soc. Mass Spectrom.* **12**, 1296–1301.

Nemirovskiy, O. V., Ramanathan, R. & Gross, M. L. 1997 Investigation of calcium induced noncovalent association of calmodulin with melittin by ESI-MS. *J. Am. Soc. Mass Spectrom.* **8**, 809–812.

Nemirovskiy, O. V., Giblin, D. E. & Gross, M. L. 1999 ESI-MS and H/D exchange for probing the interaction of calmodulin with calcium. *J. Am. Soc. Mass Spectrom.* **10**, 711–718.

Nousiainen, M., Feng, P. X., Vainiotalo, P. & Derrick, P. J. 2001 Calmodulin-RS20-Ca_4 complex in the gas-phase: electrospray ionisation and Fourier transform ion cyclotron resonance. *Eur. J. Mass Spectrom.* **7**, 393–398.

Nousiainen, M., Derrick, P. J., Lafitte, D. & Vainiotalo, P. 2003 Relative affinity constants by ESI FTICR MS: calmodulin binding to peptide analogs of myosin light chain kinase. *Biophys. J.* **85**, 491–500.

Persechini, A., McMillan, K. & Leakey, P. 1994 Activation of myosin light chain kinase and nitric oxide synthase activities by calmodulin fragments. *J. Biol. Chem.* **269**, 16 148–16 154.

Rhoads, A. R. & Friedberg, F. 1997 Sequence motifs for calmodulin recognition. *FASEB J.* **11**, 331–340.

Robinson, C. V. 2002 Characterisation of multiprotein complexes by mass spectrometry. In *Protein–protein interactions: a molecular cloning manual* (ed. E. A. Golemis), ch . 12, pp. 227–240. Cold Spring Harbor, NY: Cold Spring Harbor Laboratory.

Robinson, C. V., Chung, E. W., Kragelund, B. B., Knudsen, J., Aplin, R. T., Poulsen, F. M. & Dobson, C. M. 1996 Probing the nature of non-covalent interactions by mass-spectrometry. A study of protein-CoA ligand binding and assembly. *J. Am. Chem. Soc.* **118**, 8646–8653.

Rogniaux, H. *et al.* 1999 Binding of aldose redusctase inhibitors: correlation of crystallographic and mass spec studies. *J. Am. Soc. Mass Spectrom.* **10**, 635–647.

Schulz, D. M., Ihling, C., Clore, G. M. & Sinz, A. 2004 Mapping the topology and determination of a low-resolution three-dimensional structure of the camodulin–melittin complex by chemical cross-linking and high-resolution FT-ICR-MS: direct observation of multiple binding modes. *Biochemistry* **43**, 4703–4715.

Smith, R. D. & Whitesides, G. M. 1995 Using ESI FT-ICR-MS to study competitive binding of inhibitors to carbonic anhydrase. *J. Am. Chem. Soc.* **117**, 8859–8860.

Taylor, P. K., Kurtz, D. M. & Amster, I. J. 2001 ESI-FTICR-MS of multimeric-metalloproteins. *Int. J. Mass Spectrom.* **210/211**, 651–663.

Tsui, V. & Case, D. A. 2000 Molecular dynamics simulations of nucleic acids with a generalized Born solvation model. *J. Am. Chem. Soc.* **122**, 2489–2498.

Veenstra, T. D., Johnson, K. L., Tomlinson, A. J., Naylor, S. & Kumar, R. 1997 ESI-MS temperature effects on metal ion:protein stoichiometries and metal-induced conformational changes in Calmodulin. *Eur. J. Mass Spectrom.* **3**, 453–459.

Vorherr, T., Knopfe1, L., Hofmann, F., Mollner, S., Pfeuffer, T. & Carafoli, E. 1993 The Calmodulin binding domain of nitric oxide synthase and adenylyl cyclase. *Biochemistry* **32**, 6081–6088.

Wigger, M., Eyler, J., Benner, S., Li, W. & Marshall, A. G. 2002 FT-ICR mass spectrometric resolution, identification and screening of non-covalent complexes of Hck-Src homolgy 2 domain receptor and ligands from a 324 member peptide combinatorial library. *J. Am. Soc. Mass Spectrom.* **1213**, 1162–1169.

Xu, N., Pasa-Tolic, L., Smith, R. D., Ni, S. & Thrall, B. D. 1999 ESI-MS study of the interaction of cisplatin-adducted oligonucleotides with human XPA minimal binding protein domain. *Anal. Biochem.* **272**, 26–33.

The electronic supplementary material is available at http://dx.doi.org/10.1098/rsif.2005.0055 or via http://www.journals.royalsoc.ac.uk.